Computational Fluid Dynamics Study of Perforated Wind Tunnel Wall Effects on Wing Characteristics

Lukman N Kerur[1] Dr.G.S.Shivshankar[2]
[1]M.Tech Student(4th Semester) [2]Professor and Head
[1,2]Department of Mechanical Engineering
[1,2]Siddaganga Insititute of Technology,Tumkur, India

Abstract— In this project, we are going to study the flow past of SSD2 airfoil which is further modified version of NACA 23012 and simulating the results. Any new airfoil characteristics are derived from extensive experimental tests. However experiments are costly. In order to get an idea of airfoil characteristics we have chosen to use CFD tools. Firstly, Computations were done on 2d section model and simulated for free stream condition. Further, the airfoil properties were studied when tested in a tunnel. The flow properties in the presence of wind tunnel walls have also been simulated using CFD tools. For this purpose rectangular wing is placed in the tunnel as wall to wall. Effects of wind tunnel wall are compared with the results of 2d free air simulation. In general wind tunnel wall effects are reduced by using perforated walls. In our present study we have done a limited study on perforated walls we do show the improved prediction with respect to perforated wall. An open air ratio of 8% has been used in the present studies and compared with the 2d free air simulation. Modelling and Simulation is done using different CFD tools.

***Key words*:** 3D Perforated Model, 2d Free Stream Model, 8% Open Air Ratio, Pressure Farfield

I. INTRODUCTION

Since from many years wind tunnels are used in various applications. Having specific purpose and limitation they range from extremely simple low speed to highly complex hypersonic versions. The main objective of the wind tunnel is to recreate the flow around the body or an object in a controlled environment. When some conditions are applied to the designed model, wind tunnel helps us to understand the flow phenomenon and forces that are expected around the body .

With certain advantages and disadvantages there are wide varieties of wind tunnels. When an object is exposed to airflow, the main objective of these wind tunnels is to reproduce the unbounded airflow nearby solid boundaries. At theoretical infinite distance the streamlines around the body would bend and becomes straight again in such cases. If the space is limited in laboratory, at some finite distance there should be wind tunnel wall or some similar boundary from a test model such that the streamlines are forced to become straight again. To ensure the artificial boundaries in wind tunnel design requires a large effort but on the test piece there is minimal effect of flow and data is collected.

Towards the end of 19th century wind tunnels were invented to improve than air flying machines. By reversing the actual method wind tunnel testing is done : Rather than mov-ing the object and air as steady, the same effect can be obtained if the object is steady and allowing the air to flow on the object with different speed. In this way a stationary observer can study the aerodynamic forces which are imposed on a flying object in action. To achieve this results various methods are used. With the different effects on the streamlines there are two types of wind tunnels Closed wind tunnel and open wind tunnel.

Fig. 1: Airfoil in free flight.

Fig. 2: Airfoil in closed wind tunnel

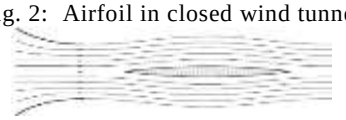

Fig. 3: Airfoil in open wind tunnel

In case of closed wind tunnel as shown in (Fig 1) the streamlines are forced to become straight because of presence of wall. At subsonic velocities there is an additional effect of increase the flow velocity around the body which causes velocity correction to be used.

In case of Open wind tunnel as shown in (Fig 3) As compared from free flight condition the streamlines tend to be more curved due to undisturbed free stream pressure is reached at the boundary of jet.

In case of perforated wall an open space region on the boundary should exist to reduce the shock effects. This open region is known as " Plenum Chamber". In open test section the shock effects are reduced and the expansion waves are formed. Plenum chamber is responsible for increase in cross sectional area around the test piece in wind tunnel. Wind tunnel choking is not due to the presence of test piece at high subsonic Mach number testing.

II. CFD SIMULATION OF WIND TUNNEL THROUGH PERFORATED WALLS

Perforations are the holes which are usually made on the top and bottom of the tunnels. They are provided in the tunnel walls for means of escape of boundary layer of air in tunnels and reduces shock wave intensity which are reflected from walls.

A. Geometry with perforated walls:

Creating the geometry with the dimensions for Upstream as 4m, Downstream as 6m, Above the wing as 3m, Below the wing as 3m and lastly wing span as 4m in Z-Direction, Chord length 1m. Give the name for each side as follows:

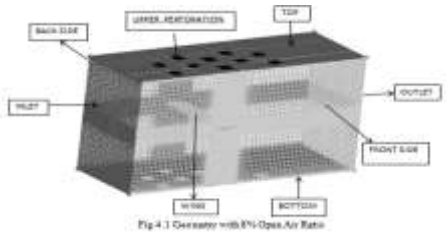

Fig.4:

B. Simulation by 8% open air ratio:

Geometry is created as shown in above fig 4, select the mesh elements and name them as Upper Perforation and Lower Perforation. To calculate the 8% Open Air Ratio steps to be carried are as follows:

Let 'X' be the area to be calculated for 10 holes and given as:

$$X * 10 = \frac{8 * 11 * 4}{100}$$

$$X * 10 = \frac{352}{100}$$

$$X * 10 = 3.52$$

$$X = \frac{3.52}{10}$$

X = 0.352 For one side

X*X = 0.352 ,

$X^2 = 0.352$

X= √0.352

X = 0.59329 which is nearly equal to 0.6

Therefore for eight percent open air ratio 0.6 is minimum area for the 10 holes. For Different percentage of open air ratio the value differs . Suppose if we are calculating for 16 percent open air ratio the area calculated for 10 holes is 0.84. Therefore the area of perforation or holes increases with increase in the percentage of open air ratio and decreases with decrease in percentage of open air ratio.

III. MESH DETAILS

SIDES	MESH ELEMENTS
BACK SIDE	24022
BOTTOM	7227
FLUID	1417298
FRONT SIDE	24022
INLET	6649
LOWER PERFORATION	520
OUTLET	11921
TOP	7203
UPPER PERFORATION	544
WING	7495
TOTAL ELEMENTS	1507155
TOTAL NODES	1461840

- Mesh quality – 0.7
- Aspect ratio – 2.57e 4
- Skewness – 0.7
- Determinant 3*3*3 – 0.871
- Orthogonal quality – 0.722

IV. BOUNDARY CONDITIONS

To define the inputs of a simulation model boundary conditions are used. The simulation of model with its surroundings are connected by boundary conditions. Without them the simulation cannot be defined and in most of the cases it cannot be proceed. Most of the boundary conditions can be defined as steady state and transient boundary conditions. Steady state boundary conditions lasts till simulation. Transient boundary conditions vary with the time and are used to simulate an event or cyclically.

The Boundary Conditions which are used for the simulation of perforated model with 8% Open air ratio are usually given in the ANSYS FLUENT Software and they are listed as follows:

A. Velocity INLET:

To define the flow velocity with all similar properties of flow at inlet , Velocity inlet boundary conditions are used. For prescribed velocity distribution the stagnation or total pressure is not fixed but will increase to the required value. Velocity boundary condition is applied to compressible and incompressible flows equally. Without the scalar inputs this boundary condition is given at the flow exit, in special cases. In the domain overall continuity is maintained in such cases. Since we are defining this boundary condition for subsonic region. Therefore the velocity inlet is calculated as :

$$M = \frac{\text{Velocity of Object}}{\text{Velocity of Sound}}$$

For Subsonic region Mach Number is 0.2 and Velocity of Sound is 346

$$0.2 = \frac{\text{Velocity Of Object}}{340}$$

Therefore, Velocity of Object = 0.2*346

Velocity of Object = 69.2 m/s

B. Pressure farfield:

At infinity to model a free steam condition with specified static condition and free stream Mach number, Pressure farfield conditions are used. To determine the flow variables at the boundaries, Pressure farfield boundary condition uses the characteristic information. Hence it is oftenly called as characteristic boundary condition.

Limitations:

Note the following limitations and restrictions when using pressure far-field boundary conditions:

- Using ideal-gas law density is calculated then the boundary condition is applied. It is not permitted to use for other flows.
- The multiphase models (Eulerian, VOF) that are available with pressure based solver are usually incompatible in nature.
- In the density based solver where the flow employs with constant density, gas model and wet steam model. The boundary condition cannot be applied.

C. Pressure outlet:

At the outlet boundary a static or gauge pressure is required to specify the Pressure outlet boundary condition. When the flow is subsonic then the value of specified gauge pressure is used. When the flow is supersonic, from the flow pressure will be extrapolated in the interior region. From interior all other flows are extrapolated.

A set of "backflow" conditions is also specified should the flow reverse direction at the pressure outlet boundary during the solution process. Convergence difficulties will be minimized if you specify realistic values for the backflow quantities. During the solution process, at the pressure outlet boundary a set of backflow conditions is also specified such that the flow reverse the direction. For the backflow quantities if the realistic values are specified difficulties will be minimised for the convergence.

D. Wall boundary condition:

To bound fluid and solid regions wall boundary conditions are used. By default no slip boundary condition is enforced at walls in case of viscous flows, but tangential velocity component can be specified in terms of rotational or translational motion of the wall boundary. (Using symmetry boundary type a slip wall with zero shear can be modified , but using the symmetry boundary condition will apply symmetry for all equations)

E. Boundary conditions for perforated wind tunnel :

SIDES	BOUNDARY CONDITIONS
INLET	VELOCITY INLET
OUTLET	PRESSURE OUTLET
TOP	WALL
BOTTOM	WALL
FRONT SIDE	WALL
BACK SIDE	WALL
UPPER PERFO	PRESSURE FARFIELD
LOWER PERFO	PRESSURE FARFIELD
WING	WALL

For 8% open air ratio are simulated with different angle of attack 2,4,6,8 and these results are compared with the 2D free stream section.

Fig. 5:

V. RESULTS:

A. Pressure Distribution on the wing for different angle of attack

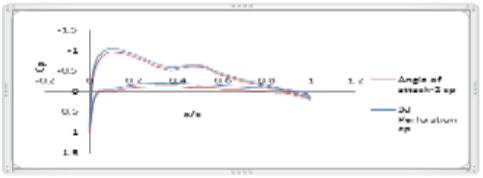

Fig. 6: Cp v/s Chord length (At Z=2) for 3d perforation and 2d free stream at 2° Angle of Attack

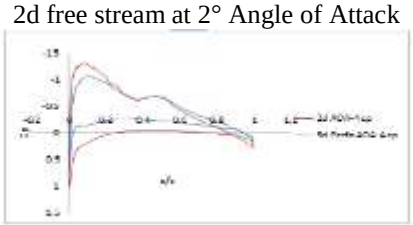

Fig. 7: Cp v/s Chord length (At Z=2) for 3d perforation and 2d free stream at 4° Angle of Attack

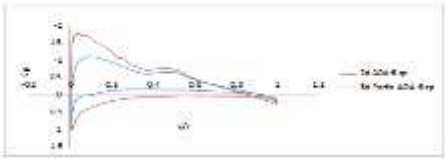

Fig. 8: Cp v/s Chord length (At Z=2) for 3d perforation and 2d free stream at 6° Angle of Attack

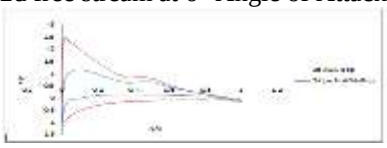

Fig. 9: Cp v/s Chord length (At Z=2) for 3d perforation and 2d free stream at 8° Angle of Attack

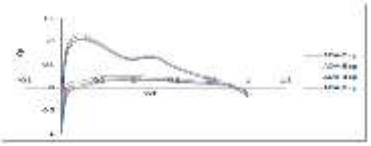

Fig. 10: Cp v/s Chord length (At Z=2) for 3d perforation for 2°, 4°, 6°,8° Angle of Attack

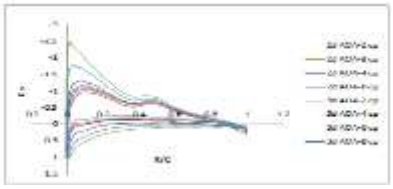

Fig. 11: Cp v/s Chord length (At Z=2) for 3d perforation and 2d free stream for 2°,4°,6°, 8° Angle of Attack

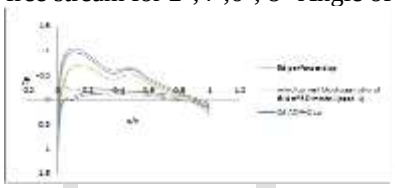

Fig. 12: Cp v/s Chord length (At Z=2) for 3d perforated, 2d and solid for 2° angle of attack

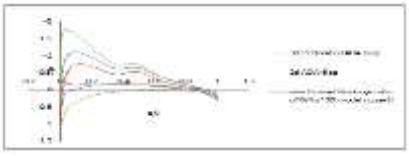

Fig. 13: Cp v/s Chord length (At Z=2) for 3d perforated, 2d and solid for 6° angle of attack

From all the above graphs it is seen that how pressure is distributed for 8% open air ratio 3d perforated model and 2d free stream with different angles of attack. Cp at the airfoil stagnation point is near to unity. It rapidly decreases at both the upper and lower surface and finally reaches the positive value at the trailing edge of the airfoil. Firstly consider 2° Angle of attack for both 3d and 2d free stream . from Fig 5 describes that the pressure distribution on the upper surface of both 3d perforated model and 2d free stream is lower than the lower surface of 3d and 2d and positive is reached at the trailing edge

From fig 6 and fig 7. for 4° and 6° angle of attack the pressure distribution on the upper surface is more for 2d as compared to 3d but at the lower surface of 2d reaches the positive value compared to 3d.

From fig 8, for 8° angle of attack the pressure distribution on the upper surface at the leading edge reaches pressure of more than -2 which is having highest peak for 2d as compared to 3d. But at the lower surface of both the 3d as well as 2d the pressure distribution is positive and at the trailing edge have the positive value.

From fig 9, the Cp v/s chord length at wing span at Z=2m the pressure distribution for different angle of attack of 2°,4°,6°,8° 3d perforated 8% open air ratio is shown. For

all the angles the pressure distribution is negative on the upper surface but for lower surface at 6° and 8° angle of attack the pressure distribution is positive.

From fig 5.6 pressure distribution for 2d and 3d for different angle of attack is shown the pressure distribution on both the lower and upper surface are compared and the results are satisfied.

From fig 10. The pressure distribution for 2d and 3d with solid model whose simulations are done by my colleague Mr. Hanumanthu in NAL. The results were compared for 2° and 6° angle of attack.

B. Lift, Drag Force and Moment at different angle of attack

Angle of attack	Cl	Cd	Cm
2	4.14e-1	1.42e-2	1.30e-01
4	5.93e-1	1.05e-2	1.62e-01
6	8.19e-1	1.19e-2	2.10e-01
8	1.03e+00	2.17e-2	2.80e-01

For 3d Perforated wind tunnel wall:

Angle of attack	Cl	Cd	Cm
2	3.95e-1	4.064e-3	1.11e-01
4	4.14e-1	1.70e-2	1.15e-01
6	4.34e-1	3.12e-2	1.19e-01
8	4.56e-1	4.68e-2	1.24e-01

For Solid wind tunnel wall (By Hanummanthu)

Angle of attack	Cl	Cd	Cm
2	1.98e-2	1.52e-2	6.93e-02
4	2.22e-2	2.22e-2	7.4e-02
6	2.40e-2	3.10e-2	7.9e-02
8	2.681e-2	4.30e-2	8.5e-02

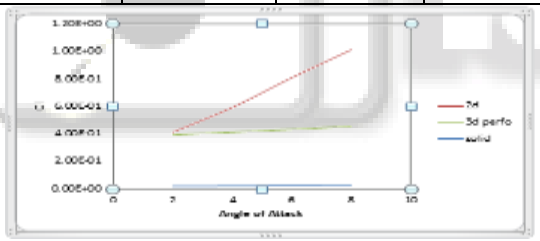

Fig. 14: Lift coefficient versus angle of attack

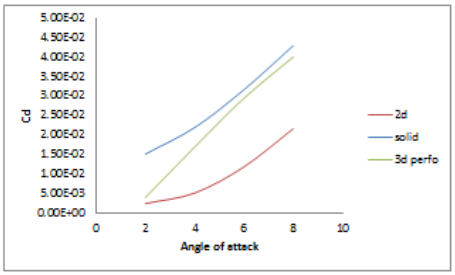

Fig. 15: Drag coefficient versus angle of attack

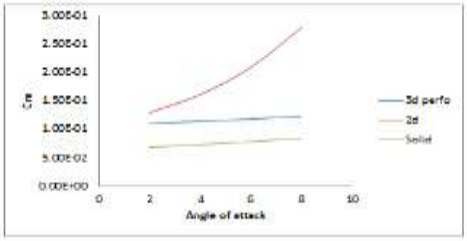

Fig. 16: Moment Coefficient versus angle of attack

From fig 18Coefficient of lift versus angle of attack, For 2d free stream condition the lift increases with the increase in angle of attack. For the 3d perforated model the lift is less as compared to 2d free stream model. For solid wall the lift is lesser than the 3d perforated model as well as 2d free stream model. The lift for 3d perforated model is close to the 2d free stream model. Hence the results are satisfied.

From fig Coefficient of drag versus angle of attack, The drag force is inversely proportional to the lift force. For solid model the drag force is more and it increases with the increase in angle of attack. For 3d perforated wall the drag force is less than solid. For 2d free stream model the drag force is less than 3d perforated model and the solid model. Since the drag force is more in the solid as compared to 3d perforated model and the results are satisfied.

From fig Pitching moment versus angle of attack, The moment force for 2d free stream model increases with the increase in angle of attack. For 3d perforated model it is less than 2d but more than solid. For solid model the moment is less than both 2d free stream as well as 3d perforated model.

VI. CONTOURS

A. Velocity contours:

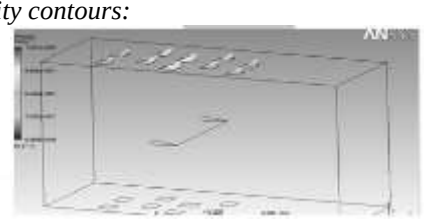

Fig. 17: Velocity Vector

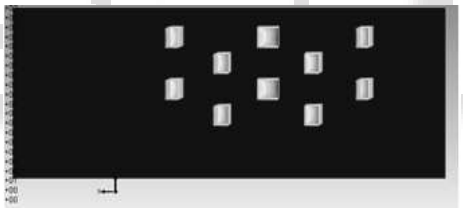

Fig. 18: Velocity magnitude (m/s)

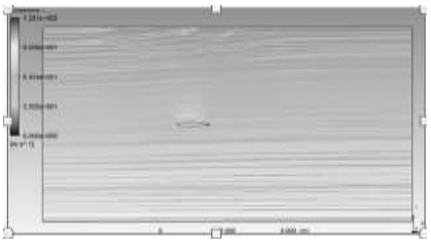

Fig. 19: Velocity streamline

From above fig the contours of velocity vector for 8% Open air ratio Perforated wind tunnel model in which the vectors are moving out through the perforations on the top. Above the airfoil the flow is more as compared to the other sides.

From above fig the contours of velocity magnitude for perforated model are shown. The velocity calculated for 0.2 Mach Number is 69.2m/s. As the fluid moves from the inlet with 69.2m/s the air escapes from the perforations with certain magnitude and is lowered at the outlet.

From above fig shows the streamlines moving out through the perforations. As the air flows from the inlet it escapes from the perforations on the top of the geometry.

Velocity streamlines shows the flow characteristics of the air on the wing as well as through the perforations.

B. Pressure Contour:

Fig. 18: Pressure near the wing

Fig. 19: Pressure near the perforations

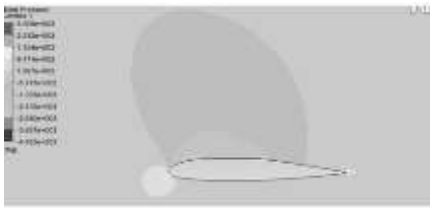

Fig. 20: Pressure on the front face

From fig 18 As the fluid flows from inlet with certain velocity and as the velocity of fluid decreases the pressure is increased and the distribution of pressure is around the wing is as shown above.

From fig 19 The flow escapes out through the 8% perforations as the flow moves out the velocity is reduced and the pressure is increased. The pressure near the perforations is as shown above.

From fig 20 For the perforated model when viewed from the front side the pressure distributed on the wing is as shown above.

VII. Conclusion

CFD flow simulation have successfully performed using ANSYS ICEM CFD and FLUENT softwares for the wind tunnel testing of Perforated walls for 8% Open air ratio using SSD2 airfoil. The Graphs for Pressure distribution, Coefficient of lift, Coefficient of drag and Pitching moment for different angle of attack were plotted and compared with the 2d free stream and the results were satisfied. The effect of pressure and velocity distribution on the perforated wind tunnel walls and the airfoil were visualized.

VIII. Scope of Future Work

- The wind tunnel testing using SSD2 airfoil for 8% open air ratio and compare this experimental results with the computational results.
- In this project we have studied the effects of perforated wind tunnel wall for 8% Blockage ratio. For the future work, have to study the perforated wall effects with the different percentage of blockage ratios.
- To study the aerodynamic characteristics for perforated wind tunnel wall with the different domain size and compute the results.

References

[1] www.nal.csir.in
[2] www.google.com
[3] "Closed-Tesi-Section Wind Tunnel Blockage Corrections for Road Vehicles."
[4] Filippone, .A... (1999-2004), "Advanced Topics in Aerodynamics." Accessed March 17, 2004. from http://aerodyn.org/WindTurmel/wind_tunnel.html
[5] Rangaraju, K.G. and Singh, V "Blockage effects on Drag of Sharp-edged Bodies." Journal of Industrial Aerodynamics (1975).
[6] Maskell, E.C. "A theory of the Blockage effect on Bluff Bodies and Stalled Wings in a closed Wind tunnel
[7] Thom, A. "Blockage correction in a closed high speed tunnel."
[8] Herriot, J.C. "Blockage correction for three dimensional flow closed throat Wind tunnel with consideration of the effect of compressibility."
[9] Ramamurthy, A.S. and Ng, CP. "Effect of Blockage on Steady Force Coefficients."' Journal of Engineering Mechanics.
[10] Awbi, H.W. 'The investigation of wind tunnel wall interference on bluff body models" Ph.D Thesis, Trent Polytechnic, Nottingham, August 1974.
[11] Awbi, H.W. "Wind-Tunnel-Wall Constraint on Two-Dimensional Rectangular-Section Prisms."' Journal of Industrial Aerodynamics.
[12] Mercker, E. "A Blockage Correction for Automotive Testing in a Wind Tunnel with Closed Test Section." Journal of Wind Engineering and Industrial Aerodynamics.
[13] Louis. G.S, "A Streamline Wind-Tunnel Working Section for Testing at High Blockage Ratios." Journal of Wind Engineering
[14] Okajima, A., Yi, D., Saliuda, A.. Nakaiio. "Numerical study of blockage effects on aerodynamic characteristics of an oscillating rectangular cylinder." Journal of Wind Engineering and industrial Aerodynamics.
[15] Perzon, S. "On Blockage Effects in Wind Tunnels - A CFD Study" Society of Automobile Engineers.
[16] Yen, J.C, Martindale. W.R, Duell, E.G, Amette, S.A. "Determining Blockage Correction in climatic Wind Tunnel, using CFD." SAE International
[17] Jeffrey, H., Bill, M., Stephen, A. (Jacobs Sverdrup), Jack, W., Stan, W. (FordMotor Company). "Development of Lift and Drag Corrections for Open Jet WindTunnel Tests for an Extended Range of Vehicle Shapes." SAE International.
[18] Launder, B.E and Spalding, D.B. "The Numerical Computation of TurbulentFlows." (1974), Computational Mechanics and Engineering.
[19] Spalding, D.B. and Zhubrin, S.V., " X-Cell: A new algorithm for fluid-flow simulation in PHOENICS." Lectures at PHOENCIS Used Conference, April 1996, Tokyo, Japan

